

# First-principles calculation of electronic spectra of light-harvesting complex II

## — Electronic supplementary information —

Carolin König and Johannes Neugebauer<sup>1</sup>

Gorlaeus Laboratories, Leiden Institute of Chemistry, Leiden University,  
P.O. Box 9502, 2300 RA Leiden, The Netherlands

---

<sup>1</sup>Email: [j.neugebauer@chem.leidenuniv.nl](mailto:j.neugebauer@chem.leidenuniv.nl)

# 1 Further structural and technical tests on isolated chloropylls

In addition to the summary in the main test, we give here a more detailed discussion of structural tests (Sec. 1.1) and the choice of the electronic structure method (Sec. 1.2).

## 1.1 Test calculations on structural effects

In this section, we discuss our test calculations on structural effects for one chlorophyll *a* (CLA, residue 601) and one chlorophyll *b* (CHL, residue 609) as examples. The results are compared to earlier experimental and theoretical studies. We analyze differences between partial and full geometry optimizations for these residues. The excitation energies and oscillator strengths for the resulting structures are shown in Table S-I.

Table S-I: Effects of different optimization strategies on the excitation energies ( $E$ ) and oscillator strengths ( $f$ ) of  $Q_y$  and  $Q_x$  band for CLA 601 and CHL 609. All structures were (partly) optimized with BP86/TZP: optA: all atoms were optimized; optR: atoms in the ring and hydrogen atoms optimized; optH: only hydrogen atoms optimized. Excitation properties were calculated with SAOP/TZP.

	$Q_y$		$Q_x$	
	$E/\text{eV}$	$f$	$E/\text{eV}$	$f$
CLA 601				
optR	1.952	0.217	2.034	0.022
optH	1.945	0.204	2.043	0.014
optA	1.951	0.219	2.034	0.022
CHL 609				
optR	1.927	0.044	1.967	0.032
optH	1.884	0.010	1.895	0.022
optA	1.923	0.043	1.963	0.033

For CLA 601 there are no significant differences in excitation properties between the optH and optA structures. In contrast to this, the calculated excitation energies and oscillator strengths of CHL 609 show considerable changes upon optimization, although the structures show no dramatic differences (see Fig. S-1). Also the shapes of the molecular orbitals are similar (not shown).

There are hardly any differences between the calculated spectra of the optR (ring atoms and hydrogens optimized) and optA structure. Therefore, the effect of structural relaxation must be attributed to geometry changes in the ring. To unravel the origin of the differences in the calculated spectra, we varied the position of the magnesium ion with

Figure S-1. Optimized structures of CHL 609. Black: optA ; red: optH.

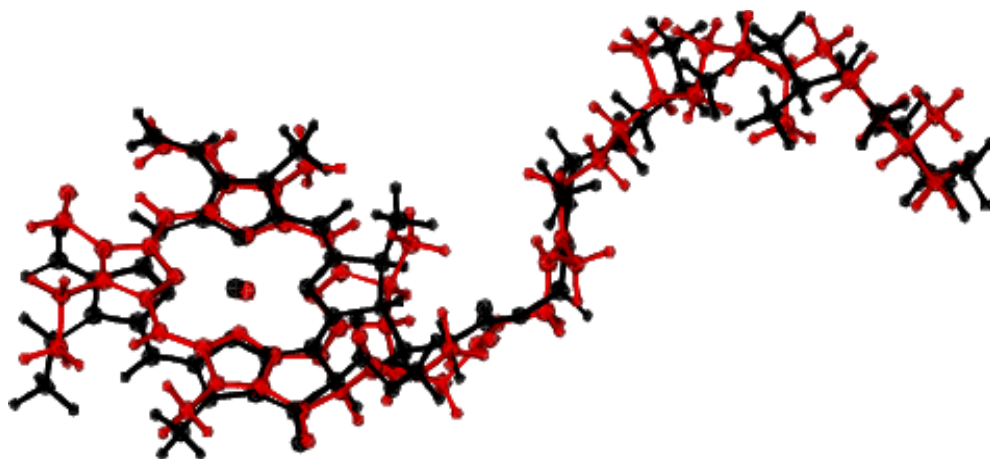


Table S-II: Calculated and experimental excitation energies ( $E/eV$ ), and oscillator strengths ( $f$ ) of  $Q_y$  and  $Q_x$  band of CHL 609 for different positions of the magnesium ion with respect to the plane of the porphyrine ring, which was approximately in  $xy$ -plane. In the optimized structure the Mg ion is located at  $z = -0.002$ .

structure	$Q_y$		$Q_x$	
	$E/eV$	$f$	$E/eV$	$f$
$z =$				
0.0	1.927	0.044	1.967	0.032
0.1	1.927	0.044	1.966	0.032
0.2	1.926	0.044	1.966	0.032
0.3	1.926	0.043	1.965	0.032
0.4	1.925	0.042	1.964	0.033
0.5	1.923	0.040	1.962	0.035

respect to the plane of the porphyrine ring. As shown in Table S-II, this does not have a significant effect on the absorption properties if no further structural changes take place. This is in agreement with the hypothesis that the position of magnesium atom itself has only a little effect on the excitation properties, which was proposed on the basis of ZINDO calculations [1,2]. These calculations predict no HOMO and LUMO contribution on the central magnesium atom. It was concluded that the main effect of the position of the magnesium is the resulting non-planar deformation.

Additionally, we tested the effect of truncating the phytol chain. For this purpose, we modified the phytol chain in CLA 601 and CHL 609 considering as models the truncated phytol chains occurring in pdb file 2BHW; the Lewis structures are given in Fig. 2 in the main text. The results for the optA structures of these models are shown in Table S-III.

For most phytol-chain models, the calculated differences in excitation energies and oscil-

Table S-III. Calculated excitation energies ( $E$ ), and oscillator strengths ( $f$ ) of  $Q_y$  and  $Q_x$  for different modifications of the phytyl chain for CHL 609 and CLA 601. The labels for the modifications are according to Fig. 2 in the main text

	$Q_y$		$Q_x$	
	$E/\text{eV}$	$f$	$E/\text{eV}$	$f$
CLA 601				
<b>C</b>	1.951	0.219	2.034	0.022
<b>D1</b>	1.952	0.220	2.034	0.022
<b>D2</b>	1.968	0.203	2.043	0.022
<b>M</b>	1.955	0.221	2.036	0.024
<b>D4</b>	1.954	0.229	2.037	0.023
CHL 609				
<b>C</b>	1.923	0.043	1.963	0.033
<b>M</b>	1.929	0.048	1.969	0.031
<b>D4</b>	1.923	0.049	1.962	0.035

lator strengths are small. The only case in which a slightly larger difference (17 meV) was observed is the lowest excitation of the **D2** derivative of CLA 601. The core structure does not show significant differences from the other models. An analysis of the orbital transition contribution shows that the HOMO→LUMO contribution to the  $Q_y$  excitation of **D2** is slightly lower and the contribution of the (HOMO−1)→(LUMO+1) transition is slightly higher than for other derivatives.

The calculated absorption properties for the fully optimized structures are compared to available experimental and earlier theoretical data in TableS-IV: The results of our calculations are consistent with former theoretical studies on chlorophyll *a* by Sundholm [3, 4]. While for the  $Q_x$  band our calculation only differs by about 0.01 eV from the previous one, the differences in the  $Q_y$  band are slightly larger. Our calculations lead to excitation energies which are about 0.05 eV lower and oscillator strengths which are about 0.4 higher. This is not surprising, since the calculations differ in several aspects like the structures, basis set, and exchange correlation (XC) functional.

In the comparison to experimental data one faces several problems: Both excitation energies and dipole strengths depend strongly on the surrounding solvent [5, 6], which is not taken into account in our calculations. The lowest excitation energy of chlorophyll *a* in diethylether differs from that in aniline by 0.04 eV [6]. Therefore, it is not surprising that the lowest two experimental excitation energies for chlorophyll *a* and the second lowest for chlorophyll *b* in  $\text{CCl}_4$  differ by more than 0.1 eV from our calculations in vacuum. The calculated excitation energy for the  $Q_y$  band fits well to the experimental one.

The dipole strengths of the  $Q_y$  band of chlorophyll *a* and chlorophyll *b* in  $\text{CCl}_4$  [7] were extrapolated to a vacuum value by Knox *et al.* [5]. The resulting values for chlorophyll *a* range from 16.3 to 22.0  $\text{D}^2$  and those for chlorophyll *b* from 9.8 to 14.7  $\text{D}^2$ , depending on the applied model. Thus, there is still a rather high uncertainty in these “experimental”

Table S-IV. Comparison of calculated and experimental excitation energies ( $E$ ), oscillator ( $f$ ), and dipole ( $d$ ) strengths for the  $Q_y$  and  $Q_x$  bands for chlorophyll  $a$  and chlorophyll  $b$ . All input geometries from this work were fully optimized (BP86/TZP).

	$E/\text{eV}$	$f$	$d/D^2$	$E/\text{eV}$	$f$	Ref.
chlorophyll $a$						
Theoretical studies						
CLA 601	1.951	0.219	29.5	2.034	0.022	this work
chl $a$ , BP86/SV(P)	1.997	0.182	24.0	2.036	0.026	[3]
CLA 601 (M)	1.955	0.221	29.9	2.036	0.024	this work
chl $a$ , phytol replaced by H BP86/SV(P)	2.000	0.186	24.5	2.043	0.027	[4]
Experimental data						
in $\text{CCl}_4$	1.864	0.225	31.8	2.141	0.064	[7]
fitted to vacuum			16.3 to 22.0			[5]
chlorophyll $b$						
Theoretical study						
CHL 609	1.923	0.043	5.8	1.963	0.033	this work
Experimental data						
in $\text{CCl}_4$	1.922	0.136	18.6	2.077	0.034	[7]
fitted to vacuum			9.8 to 14.7			[5]

values. In spite of this rather large uncertainty, the calculated values still lie outside this range. Furthermore, earlier computational studies reported that calculated oscillator strengths can vary considerably when changing the XC functional [8,9]. In case of chlorophyll  $a$ , the calculated dipole strength for the  $Q_y$  band is higher than the experimental one while the one for  $Q_x$  is lower. For the  $Q_y$  band of chlorophyll  $b$  we calculated a lower intensity than found in experiment. But the experimental and calculated values for the oscillator strength of the  $Q_x$  band of this chlorophyll molecule agree well. This demonstrates that TDDFT gives reasonable results for excitation energies and oscillator strengths of chlorophylls.

## 1.2 Choice of the electronic-structure method

As a next step, we investigated the sensitivity of the relative  $Q_y$  excitation energies to a change in the applied electron-structure method. This includes tests of the effects of the Tamm-Dancoff approximation (TDA) and of varying the XC functional. We employed the DFT model potential SAOP, the hybrid functional B3LYP and the double hybrid functional B2PLYP. The latter was shown to give better excitation energies than normal hybrid functionals in many cases [10]. In addition, we calculated the excitation energies using CIS and CIS(D).

Table S-V. Calculated excitation energies ( $E/eV$ ) of the  $Q$  bands band of all chlorophyll pigments in chain A, modified according to structure **M** in Fig. 2 for optH structures using SAOP/TZP with and without TDA.

residue	no TDA		TDA	
	$Q_y$	$Q_x$	$Q_y$	$Q_x$
CLA 601	1.945	2.048	2.097	2.122
CLA 602	1.907	2.047	2.061	2.108
CLA 603	1.940	2.049	2.083	2.124
CLA 604	1.954	2.067	2.105	2.144
CLA 605	1.912	2.029	2.061	2.091
CLA 606	1.967	2.066	2.113	2.130
CLA 607	1.895	2.013	2.034	2.077
CLA 608	1.895	1.997	2.035	2.063
CHL 609	1.886	1.899	1.983	1.956
CHL 610	1.900	1.934	2.009	1.991
CHL 611	1.867	1.896	1.967	1.940
CHL 612	1.900	1.912	1.989	1.966
CHL 613	1.912	1.960	2.042	2.014
CHL 614	1.891	1.917	1.996	1.972

For the SAOP potential, we carried out calculations with and without the TDA. The excitation energies and oscillator strengths for the  $Q$  bands of all chlorophyll pigments (optH) are shown in Table S-V. Applying the TDA in general leads to higher excitation energies. It turns out that the shifts for a particular  $Q$  excitation in one class of chlorophylls is rather systematic: For CLA, the calculated  $Q_y$  excitation energies are 0.139 (CLA 607) to 0.154 eV (CLA 602) higher if the TDA is employed. The differences for the  $Q_x$  excitation energies lie in the range from 0.061 (CLA 603) to 0.077 eV (CLA 604). For CHL residues the  $Q_y$  differences amount to between 0.089 (CHL 612) and 0.109 eV (CHL 610) and the  $Q_x$  differences to between 0.044 (CHL 611) and 0.057 eV (CHL 609 and CHL 610). Hence, the  $Q_y$  excitation energies of the CHL residues are lowered relative to those of the CLA residues if the TDA is applied. Additionally, the sensitivity to the TDA is more pronounced for the  $Q_y$  than for the  $Q_x$  excitations. This leads to a decreased  $Q_x-Q_y$  energy difference if the TDA is employed. For the CLA residues, the calculated  $Q_x-Q_y$  differences lie between 0.099 eV for CLA 606 and 0.140 eV for CLA 602. If the TDA is applied, the differences shrink to 0.017 and 0.047 eV, respectively, for the same residues. For CHL residues, this effect even reverses the energetic order of the two  $Q$  excitations: Without TDA, they lie between 0.013 (CHL 609) and 0.048 eV (CHL 613) and with TDA between  $-0.018$  (CHL 610) and  $-0.028$  eV (CHL 613).

Also the oscillator strengths are sensitive to the application of the TDA, but there is no clear trend in direction or magnitude of these changes. The mixing of the  $Q_y$  and the  $Q_x$  excitations tends to be more pronounced when the TDA is applied. This effect is more distinct for the CHL than for the CLA residues. An example is CHL 611: The

Table S-VI. Calculated excitation energies ( $E/\text{eV}$ ) of the  $Q$  bands using CIS and CIS(D), respectively and a TZVP basis set for optH input structures.

residue	CIS		CIS(D)	
	$Q_y$	$Q_x$	$Q_y$	$Q_x$
CLA 601	2.270	3.188	2.214	2.254
CLA 602	2.232	3.098	2.181	2.280
CLA 603	2.213	3.061	2.240	2.282
CLA 604	2.259	3.135	2.249	2.277
CLA 605	2.243	3.106	2.199	2.257
CLA 606	2.283	3.206	2.241	2.272
CLA 607	2.199	2.983	2.196	2.244
CLA 608	2.235	3.091	2.193	2.235
CHL 609	2.355	3.237	2.170	2.180
CHL 610	2.352	3.244	2.203	2.206
CHL 611	2.337	3.194	2.173	2.173
CHL 612	2.366	3.200	2.206	2.173
CHL 613	2.298	3.193	2.196	2.211
CHL 614	2.333	3.224	2.179	2.170

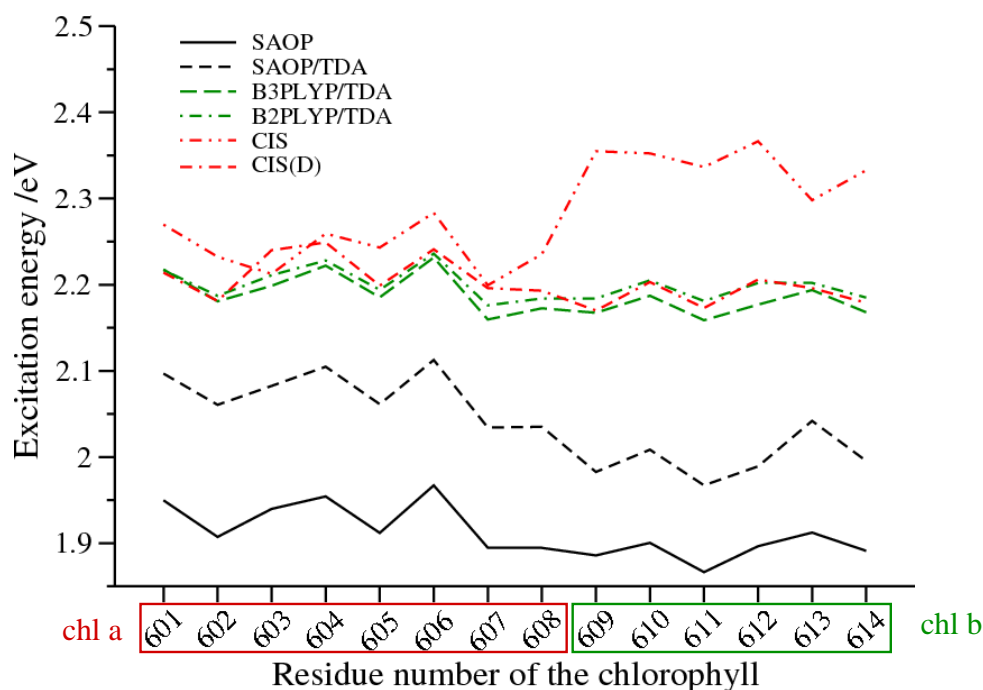
TDDFT calculation leads to 66% HOMO–LUMO contribution to the  $Q_y$  excitation. This is reduced to 32%, when the TDA is employed. It is accompanied by a redistribution of the oscillator strengths of the  $Q$  bands. While the sum stays approximately the same, the  $Q_y/Q_x$  ratio is reduced from 5.05 to 1.73.

In Table S-VI, the two lowest excitation energies calculated using CIS and CIS(D) are shown for each pigment. When comparing the  $Q_y$  and the  $Q_x$  excitation energies obtained with these two methods, it is striking that the  $Q_x$  excitations are lowered by approximately 1 eV when the perturbative second-order correction is employed. This decrease even leads to a reversed energetical order of the two  $Q$  bands for some chlorophyll structures, namely CLA 602, CHL 612, and CHL 614.

A comparison of the excitation energies obtained with different electronic–structure methods for the isolated chlorophyll pigments in LHC II is given in Fig. S-2. Here it can be seen that the absolute excitation energies are increased if (double) hybrid functionals are employed. The  $Q_y$  excitation energies obtained by CIS lie even higher. This difference is much more pronounced for the CHL than for the CLA residues. The CIS(D) results are in most cases slightly higher than the ones obtained with (double) hybrid functionals but below those calculated with CIS. Although the absolute  $Q_y$  excitation energies differ by up to 0.047 eV, the relative excitation energies are approximately the same for all applied methods within the set of CLA or CHL molecules.

CIS is the only among the tested methods which reproduces the experimentally known trend that the  $Q_y$  excitation energies are higher for CHL than for CLA (see, e.g., Ref. [11]). This finding is in line with the dependence of the  $Q_y$  excitation energies on the percentage

Figure S-2: Comparison of the excitation energies obtained for optH structures and with different electronic-structure methods for the isolated chlorophyll pigments.



of the Hartree-Fock exchange in the XC functional for CLA and CHL observed in Ref. [12] since the CIS method can be regarded as a TDA to time-dependent Hartree-Fock (100% exact exchange). But if CIS(D) is applied, a rather good agreement with the results from the (double) hybrid functionals is obtained. Furthermore, the relative excitation energies calculated with CIS(D) are quite similar to those calculated with TDDFT/SAOP. Since the same also holds for the relative energies from the (double) hybrid functionals, this justifies the use of the SAOP potential in our calculations.

## 2 Possible charge-leaking effects in the FDE calculations

As outlined in the main text, introduction of a negative charge close to the chlorophyll in the test environment model CLA 601 has a large effect on the  $Q$  excitations. The HOMO of the charged residue (not shown) exhibits a small distortion towards the chlorophyll molecule. This could be due to a normal polarization effect but it might also indicate a weak charge-leaking effect towards the chlorophyll [13–16], which can affect the energy and the composition of the electronic transition.

One way of curing this problem in FDE is to apply a long-distance correction to the kinetic-energy component of the embedding potential [15]. In the present example, this leads to a change in excitation energy of 0.015 eV for the charged model and of up to 0.007 eV for the neutral models. From this it could be argued that a weak charge leaking effect is present in the calculation, which is more pronounced for the charged model. In view of the minor changes, however, this can be considered a normal polarization effect. The changes in excitation energies, oscillator strengths (see Table S-VII), and contributions to the excitations (see Table S-VIII) due to this correction are small compared to those induced by the charged environment. Hence, the overall picture of the differences between the neutral and the charged environment is not affected by the long-distance correction.

Table S-VII: Extended version of Table I in the main text, listing also the results for CLA 601 (a)–(c) [see Fig. 4 in the main text] obtained with the long–distance correction [15].

	$Q_y$		$Q_x$	
	$E/\text{eV}$	$f$	$E/\text{eV}$	$f$
isolated pigments				
CLA 601	1.941	0.210	2.047	0.015
CLA 602	1.902	0.203	2.047	0.009
CLA 603	1.941	0.221	2.056	0.014
CLA 607	1.892	0.188	2.013	0.007
models including a test environment				
CLA 601 (a)	1.912	0.196	1.997	0.023
long–distance corrected	1.916	0.199	2.004	0.021
CLA 601 (b)	1.826	0.068	1.905	0.165
long–distance corrected	1.841	0.082	1.909	0.152
CLA 601 (c)	1.904	0.176	1.968	0.057
long–distance corrected	1.910	0.186	1.975	0.047
CLA 603	1.927	0.213	2.009	0.024
CLA 602	1.860	0.180	1.964	0.042
CLA 607	1.872	0.175	1.970	0.008
CLA 602 and CLA 607				
FDEc	1.843	0.324	1.963	0.024
	1.886	0.043	1.971	0.022
super	1.818	0.315	1.920	0.018
	1.843	0.074	1.971	0.010

Table S-VIII: Contributions of transitions between frontier orbitals to the  $Q$  bands of CLA 601 for the isolated pigment, for neutral minimal environment (a) and (c) as well as for the negatively charged ligand (b). The minimal environment was included in terms of FDEu calculations including three freeze-and-thaw cycles. (b)\* denotes a calculation on model (b) with a long-distance correction to the embedding potential (see main article for details).

			isolated	(a)	(c)	(b)	(b)*
$Q_y$							
HOMO	→	LUMO	0.838	0.805	0.773	0.440	0.489
HOMO-1	→	LUMO+1	0.124	0.094	0.078	0.023	0.030
HOMO-1	→	LUMO	0.001	0.001	0.054	0.412	0.362
HOMO	→	LUMO+1	0.001	< 0.001	0.007	0.053	0.048
$Q_x$							
HOMO	→	LUMO	0.002	< 0.001	0.049	0.395	0.349
HOMO-1	→	LUMO+1	< 0.001	< 0.001	0.018	0.070	0.065
HOMO-1	→	LUMO	0.717	0.758	0.744	0.414	0.461
HOMO	→	LUMO+1	0.250	0.164	0.159	0.086	0.095

### 3 Additional Tables and Figures

Figure S-3: Simulated absorption spectra of the two lowest excitations of CHL 601 within a minimal environment for different freeze-and-thaw cycles. The Gaussian line shape is modeled assuming a half width of 0.01 eV.

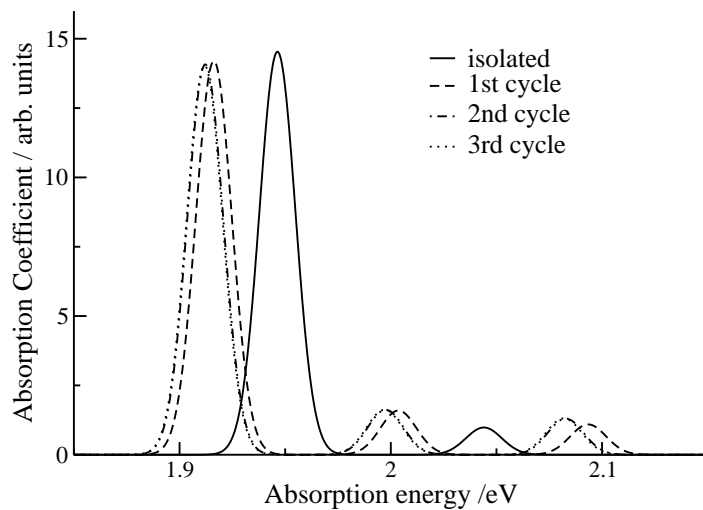


Figure S-4: Frontier orbitals for the chlorophyll pigment in the minimal environment models (a) and (b) for CLA 601 obtained in the FDEu calculations.

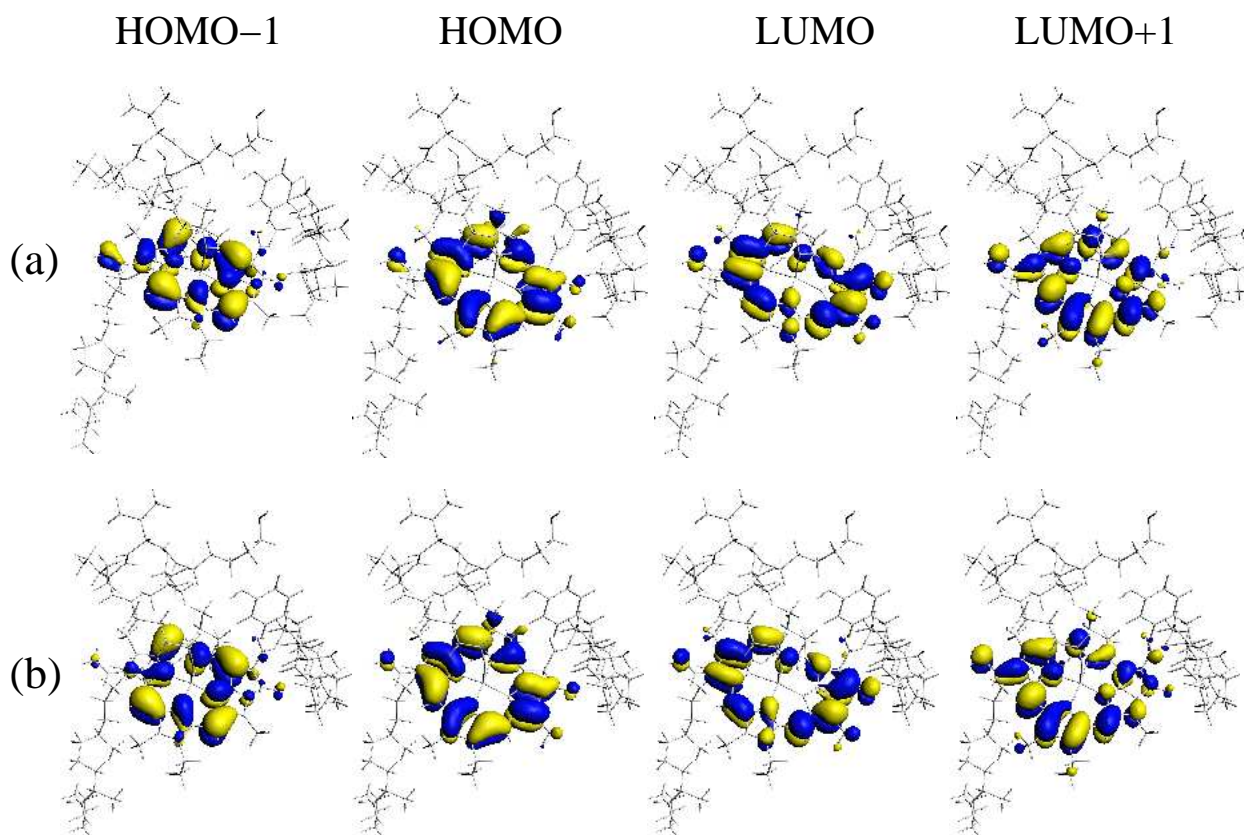


Table S-IX: Calculated  $Q_y$  and  $Q_x$  excitation energies  $E/eV$  and oscillator strengths  $f$  for all chlorophyll pigments in chain A with minimal environment (see Fig. 7 in the main article) within the FDEu approach (SAOP/TZP). In some cases the assignment of the  $Q$  bands is not unambiguous \*Strongly mixing  $Q$  states with a contribution of the other state larger than around 0.30. (H = HOMO, L = LUMO).

residue	$Q_y$				$Q_x$			
	$E/eV$	$f$	H→L	H-1→L+1	$E/eV$	$f$	H-1→L	H→L+1
<b>optH</b>								
CLA 601	1.937	0.204	0.83	0.11	2.004	0.033	0.75	0.21
CLA 602	1.882	0.185	0.83	0.09	1.991	0.033	0.68	0.25
CLA 603	1.925	0.214	0.83	0.13	1.995	0.023	0.75	0.21
CLA 604	1.899	0.227	0.85	0.09	1.944	0.034	0.80	0.15
CLA 605	1.903	0.199	0.84	0.11	1.985	0.017	0.71	0.25
CLA 606	1.946	0.222	0.85	0.12	2.048	0.014	0.70	0.26
CLA 607	1.883	0.182	0.83	0.14	1.981	0.008	0.68	0.29
CLA 608	1.882	0.164	0.78	0.11	1.955	0.034	0.66	0.25
CHL 609	1.864	0.073	0.45	0.21	1.836	0.026	0.30	0.38
CHL 610	1.887	0.125	0.73	0.18	1.895	0.015	0.37	0.60
CHL 611*	1.843	0.076	0.39	0.21	1.814	0.037	0.29	0.27
CHL 612	1.873	0.082	0.63	0.29	1.855	0.019	0.34	0.60
CHL 613	1.906	0.158	0.72	0.19	1.932	0.020	0.38	0.55
CHL 614	1.869	0.104	0.68	0.26	1.855	0.008	0.42	0.54
<b>optA</b>								
CLA 601	1.935	0.225	0.82	0.14	1.972	0.028	0.78	0.16
CLA 602	1.975	0.165	0.76	0.10	2.003	0.068	0.70	0.16
CLA 603	1.962	0.188	0.78	0.12	1.988	0.063	0.74	0.17
CLA 604*	1.924	0.181	0.52	0.10	1.928	0.084	0.52	0.07
CLA 605	1.967	0.194	0.81	0.15	2.004	0.027	0.76	0.20
CLA 606	1.952	0.224	0.83	0.13	2.029	0.030	0.75	0.20
CLA 607*	1.978	0.193	0.51	0.09	1.918	0.057	0.51	0.09
CLA 608	1.973	0.193	0.80	0.15	2.001	0.025	0.75	0.19
CHL 609	1.931	0.066	0.61	0.29	1.889	0.005	0.58	0.33
CHL 610	1.925	0.053	0.52	0.25	1.881	0.010	0.51	0.28
CHL 611	1.935	0.049	0.43	0.20	1.887	0.022	0.42	0.23
CHL 612	1.910	0.030	0.37	0.24	1.847	0.009	0.45	0.18
CHL 613	1.934	0.062	0.43	0.27	1.978	0.027	0.37	0.31
CHL 614	1.924	0.039	0.50	0.32	1.869	0.006	0.52	0.31

Table S-X: Calculated excitation energies  $E$  and oscillator strength  $f$  for  $Q_y$  and  $Q_x$  for all chlorophyll pigments in chain A with minimal environment (see Fig. 7) for the supersystem calculation (SAOP/TZP). For comparison the frontier orbitals correspond to those of the isolated chlorophylls and not of the total system (H = HOMO, L = LUMO). In some cases (indicated by a \*) this assignment is not unambiguous. In the super calculation for CHL 609 the HOMO+1 is so widely spread, that no contribution is assigned. †Strongly mixing  $Q$  states with a contribution of the other state larger than 0.20.

residue	$Q_y$				$Q_x$			
	$E/eV$	$f$	H→L	H-1→L+1	$E/eV$	$f$	H-1→L	H→L+1
<b>optH</b>								
CLA 601	1.923	0.202	0.83	0.10	1.986	0.038	0.74	0.19
CLA 602	1.879	0.174	0.82	0.09	1.982	0.034	0.70	0.24
CLA 603	1.908	0.219	0.83	0.12	1.960	0.019	0.71	0.16
CLA 604*	1.874	0.259	0.76	0.07	1.922	0.028	0.71	0.12
CLA 605	1.896	0.187	0.83	0.12	1.953	0.016	0.74	0.22
CLA 606	1.944	0.240	0.76	0.11	2.048	0.014	0.69	0.28
CLA 607	1.858	0.184	0.84	0.12	1.971	0.007	0.69	0.28
CLA 608†	1.868	0.118	0.64	0.09	1.920	0.069	0.57	0.18
CHL 609*	1.873	0.045	0.23	0.24	1.811	0.015	0.35	0.18
CHL 610	1.882	0.100	0.52	0.14	1.884	0.040	0.29	0.42
CHL 611†	1.815	0.066	0.42	0.07	1.836	0.063	0.33	0.25
CHL 612†	1.861	0.056	0.34	0.16	1.837	0.024	0.28	0.29
CHL 613	1.921	0.145	0.73	0.20	1.949	0.014	0.40	0.55
CHL 614	1.861	0.074	0.63	0.25	1.844	0.003	0.50	0.43
<b>optA</b>								
CLA 601	1.928	0.230	0.82	0.13	1.964	0.027	0.78	0.16
CLA 602	1.970	0.148	0.74	0.10	2.000	0.050	0.47	0.12
CLA 603	1.954	0.180	0.78	0.11	1.979	0.057	0.67	0.13
CLA 604	1.907	0.251	0.77	0.11	1.917	0.034	0.78	0.11
CLA 605	1.961	0.182	0.81	0.15	1.989	0.026	0.77	0.19
CLA 606	1.949	0.245	0.83	0.13	2.029	0.030	0.75	0.20
CLA 607†	1.963	0.185	0.45	0.07	1.903	0.070	0.46	0.05
CLA 608	1.968	0.182	0.75	0.15	1.988	0.024	0.75	0.18
CHL 609*	1.950	0.060	0.44		1.902	0.008	0.37	
CHL 610	1.919	0.056	0.52	0.26	1.875	0.008	0.52	0.28
CHL 611	1.930	0.058	0.44	0.21	1.881	0.021	0.43	0.23
CHL 612†	1.904	0.037	0.38	0.24	1.841	0.008	0.46	0.19
CHL 613	1.932	0.580	0.41	0.27	1.976	0.028	0.36	0.31
CHL 614	1.914	0.357	0.49	0.32	1.861	0.005	0.50	0.31

Figure S-5: Calculated (SAOP/TZP) stick and broadened spectra for the complete chlorophyll network in chain A with FDEu and FDEc.

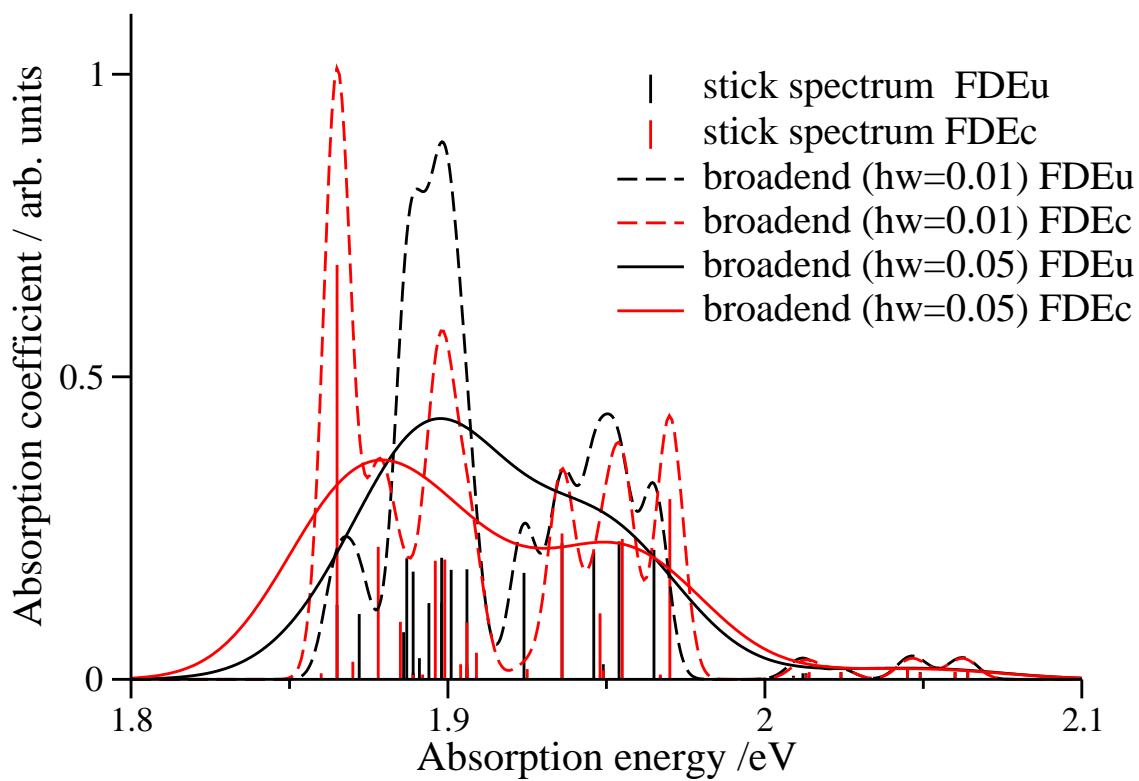


Table S-XI: Selected coupling matrix elements of the  $Q$  excitations in the FDEc calculations for all pigments in the chlorophyll network of chlorophylls in model **M** in units of meV. The letter behind the residue number (x or y) indicates to which  $Q$  excitation we refer. Additional results from earlier studies by Frähmcke *et al.* [17] and Müh *et al.* [18] are shown. For the latter, the values in parenthesis are those calculated on the basis of the crystal structure by Standfuss *et al.* [19] in case they differ significantly from those calculated for the crystal structure reported by Liu *et al.* [20]. Only coupling constants are shown whose absolute values are  $\geq 5$  in a least one of the studies.

	602y	605y	607y	607x	608	609y	610y	611y	612y	613y	613x	614y	614x
601y	-5	—	7	—	—	—	—	<b>11</b>	—	—	—	—	—
[17]	2	—	3	—	—	—	—	<b>7</b>	—	—	—	—	—
[18]	2	—	3	—	—	—	—	<b>5</b>	—	—	—	—	—
								<b>(6)</b>					
602y	—	—	<b>22</b>	—	—	—	—	—	—	—	—	—	—
[17]	—	—	<b>13</b>	—	—	—	—	—	—	—	—	—	—
[18]	—	—	<b>12</b>	—	—	—	—	—	—	—	—	—	—
			<b>(15)</b>										
602x	—	—	—	2	—	—	—	—	—	—	—	—	—
[17]	—	—	—	5	—	—	—	—	—	—	—	—	—
603y	—	—	—	—	-2	—	—	—	—	—	—	—	—
[17]	—	—	—	—	3	—	—	—	—	—	—	—	—
[18]	—	—	—	—	-4	—	—	—	—	—	—	—	—
					<b>(-6)</b>								
604y	-6	—	—	—	—	<b>11</b>	—	—	5	—	—	—	—
[17]	n.g.	—	—	—	—	<b>6</b>	—	—	3	—	—	—	—
[18]	2	—	—	—	—	<b>4</b>	—	—	-3	—	—	—	—
604x	—	—	—	—	—	-5	—	—	—	—	—	—	—
[17]	—	—	—	—	—	1	—	—	—	—	—	—	—
605y	—	—	—	—	—	—	—	—	<b>10</b>	—	—	—	—
[18]	—	—	—	—	—	—	—	—	<b>9</b>	—	—	—	—
606y	—	—	—	—	—	—	-5	—	—	<b>20</b>	0	—	—
[17]	—	—	—	—	—	—	2	—	—	<b>10</b>	7	—	—
[18]	—	—	—	—	—	—	3	—	—	<b>9</b>	n.g.	—	—
606x	—	—	—	—	—	—	—	—	—	-4	—	—	—
[17]	—	—	—	—	—	—	—	—	—	8	—	—	—
607y	—	—	—	—	—	5	—	—	—	—	—	—	—
[17]	—	—	—	—	—	2	—	—	—	—	—	—	—
[18]	—	—	—	—	—	2	—	—	—	—	—	—	—
610y	—	—	—	—	—	—	—	—	—	-6	4	—	—
[17]	—	—	—	—	—	—	—	—	—	3	6	—	—
[18]	—	—	—	—	—	—	—	—	—	2	n.g.	—	—
610x	—	—	—	—	—	—	—	—	—	5	—	—	—
612y	—	—	—	—	—	—	—	—	—	5	—	—	—
[18]	—	—	—	—	—	—	—	—	—	0	—	—	—
612x	—	—	—	—	—	—	—	—	—	8	—	—	—
613y	—	—	—	—	—	—	—	—	—	—	—	-6	2
[17]	—	—	—	—	—	—	—	—	—	—	—	1	5
[18]	—	—	—	—	—	—	—	—	—	—	—	1	n.g.

Table S-XII: Mixing between selected pairs of pigments in the whole complex and in the mutant lacking a pigment which was proposed to be a bridging pigment in Section 3.5 of the main article.

pigments		bridged by	mixing/%			
A	B		whole		mutant	
			A in B	B in A	A in B	B in A
602	609	607	19	41	<1	<1
602	611	601	15	8	1	2
610	614	613	24	34	1	1
611x	613	612	30	13	5	3
612x	614	613	31	14	<1	<1

## References

- [1] J. Linnato and J. Korppi-Tommola, *Phys. Chem. Chem. Phys.* **8**, 663 (2006).
- [2] J. Linnato and J. Korppi-Tommola, *J. Comput. Chem.* **25**, 123 (2004).
- [3] D. Sundholm, *Chem. Phys. Lett.* **302**, 480 (1999).
- [4] D. Sundholm, *Chem. Phys. Lett.* **317**, 545 (2000).
- [5] R. S. Knox and B. Q. Spring, *Photochem. Photobiol.* **77**, 497 (2003).
- [6] G. R. Seely and R. G. Jensen, *Spectrochim. Acta* **21**, 1835 (1965).
- [7] K. Sauer, J. R. L. Smith, and A. J. Schultz, *J. Am. Chem. Soc.* **88**, 2681 (1966).
- [8] M. Miura, Y. Aoki, and B. Champagne, *J. Chem. Phys.* **127**, 084103 (2007).
- [9] J. Adolphs, F. Müh, M. E. Madjet, M. Schmidt am Busch, and T. Renger, *J. Am. Chem. Soc.* **132**, 3331 (2010).
- [10] S. Grimme and F. Neese, *J. Chem. Phys.* **127**, 154116 (2007).
- [11] H. Scheer, editor, *Chlorophylls*, CRC Press, Boca Raton, Florida, USA, 1991.
- [12] T. Renger, M. E. Madjet, F. Müh, I. Trostmann, F.-J. Schmitt, C. Theiss, H. Paulsen, H. J. Eichler, A. Knorr, and G. Renger, *J. Phys. Chem. B* **113**, 9948 (2009).
- [13] A. Laio, J. VandeVondele, and U. Rothlisberger, *J. Chem. Phys.* **116**, 6941 (2002).
- [14] C. R. Jacob, T. A. Wesolowski, and L. Visscher, *J. Chem. Phys.* **123**, 174104 (2005).
- [15] C. R. Jacob, S. M. Beyhan, and L. Visscher, *J. Chem. Phys.* **126**, 234116 (2007).
- [16] S. Fux, K. Kiewisch, C. R. Jacob, J. Neugebauer, and M. Reiher, *Chem. Phys. Lett.* **461**, 353 (2008).
- [17] J. S. Frähmcke and P. J. Walla, *Chem. Phys. Lett.* **430**, 397 (2006).
- [18] F. Müh, M. E. Madjet, and T. Renger, *J. Phys. Chem. B* **114**, 13517 (2010).
- [19] J. Standfuss, A. C. Terwisscha van Scheltinga, M. Lamborghini, and W. Kühlbrand, *EMBO J.* **24**, 919 (2005).
- [20] Z. Liu, H. Yan, K. Wang, T. Kuang, J. Zhang, L. Gui, X. An, and W. Chang, *Nature* **428**, 287 (2004).